Zeitschrift: IABSE congress report = Rapport du congrès AIPC = IVBH Kongressbericht

Band: 13 (1988)

Artikel: Application of friction damper to highrise buildings

Autor: Teramoto, Takayuki / Kitamura, Haruyuki / Araki, Kenji

DOI: https://doi.org/10.5169/seals-13078

Application of Friction Damper to Highrise Buildings

Application d'un amortisseur à friction pour un gratte-ciel

Anwendung von Reibungsdämpfern in Hochbauten

Takayuki TERAMOTO
Chief Struct. Eng.
Nikken Sekkei Ltd.
Tokyo, Japan

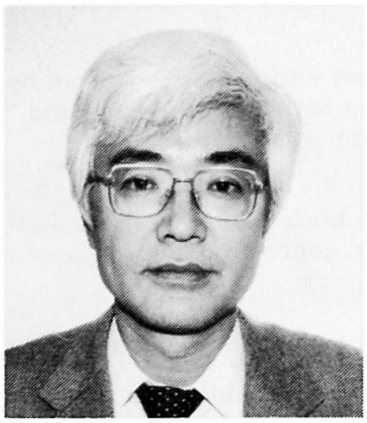

Takayuki Teramoto, born 1948, obtained his master of engineering at the Tokyo Institute of Technology, JAPAN. He was involved in the structural design of mainly highrise buildings. He is now the Chief of Structural Department of the firm.

Haruyuki KITAMURA
Senior Struct. Eng.
Nikken Sekkei Ltd.
Tokyo, Japan

Kenji ARAKI
Assist. to Gen. Mgr.
Sumitomo Metal Industries, Ltd.
Osaka, Japan

Kiichi TAKADA
Res. Eng.
Sumitomo Metal Industries Ltd.
Tokyo, Japan

SUMMARY
This paper introduces the fundamental characteristics of a new type of friction damper and describes some experiments of the damper itself and a frame with a damper under static and dynamic loading. The friction dampers are used in the highrise building in order to decrease horizontal displacements caused by earthquakes.

RÉSUMÉ
Ce papier pésente les caractéristiques fondamentales d'un nouveau type d'amortisseur à friction et décrit quelques essais de l'amortisseur lui-même et d'un encadrement avec un amortisseur sous une charge statique et dynamique. Les amortisseurs à friction sont utilisés dans un édifice à 31 étages afin de diminuer des déplacements horizontaux occasionnés par des secousses sismiques.

ZUSAMMENFASSUNG
Die vorliegende Abhandlung erklärt die Grundeigenschaften eines neuen Reibungsdämpfertyps und beschreibt Versuche, mit diesem Dämpfer allein und im Zusammenhang mit einem Bauwerk unter statischen und dynamischen Belastungen. Diese Reibungsdämpfer werden in einem 31 Stockwerke hohen Gebäude verwendet, um die Horizontalverschiebung bei Erdbeben niedrig zu halten.

1. INTRODUCTION

In the structural design of a highrise building, its seismic design is made by fully studying its expected behavior during a big earthquake. It has become hard to economically reduce the displacement during an earthquake because of its longer natural period. To reduce the building's displacement, it is effective to install dampers. The dampers effectively reduce the seismic input into the structure, finishing materials, etc., and the sway due to small- to medium-scale earthquakes or usual wind, improving the psychological effect on inhabitants of the building. Mainly to reduce the displacement and imprvove the vibration characteristics in a highrise building, friction dampers were installed on each floor and in each direction to produce certain frictional damping.

2. FRICTION DAMPER MECHANISM

Fig. 1 shows the friction damper's mechanism. The damper consists of a rod, nuts and a cup spring through which the rod passes, a friction part consisting of an inner wedge and a cotter outer wedge, and a steel outer cylinder.

The frictional force is obtained by pressing the inner wedge onto either nut by means of the cup spring and generating a compressive force between the cotter outer wedge and the steel outer cylinder interior. Its value is controlled by means of the nut tightening torque.

A piece of copper alloy is used as a friction part in the contact portion of the cotter outer wedge with the steel outer cylinder. Many pieces of solid lubricant (graphite) are imbedded to give a stable frictional force and to prevent abnormal noise generation at frictional movement. An oil-less mechanism is adopted.

2.1 Method of Test

Fig. 2 shows the method of loading. The steel outer cylinder was fixed with a pin and sine-wave vibration by deformation control was applied from the rod side. The measured items were the damper's input load (frictional force), the friction part's sliding amount, and the steel outer cylinder's temperature. The test was conducted after vibration of about 750 cycles (amplitude 1 mm, frequency 1 Hz) in order to adjust the friction face's initial condition.

Vibration was applied as shown in Table 1 to study the effects of the vibration speed, the vibration cycle and the friction face temperature on the damper's dynamic characteristics.

2.2 Test Results

A slight drop in frictional force is observed at the moment when the friction part starts sliding (e.g. the ○ mark in Fig. 3). It is considered to be a transitional phenomenon when sliding shifts from static to dynamic friction.

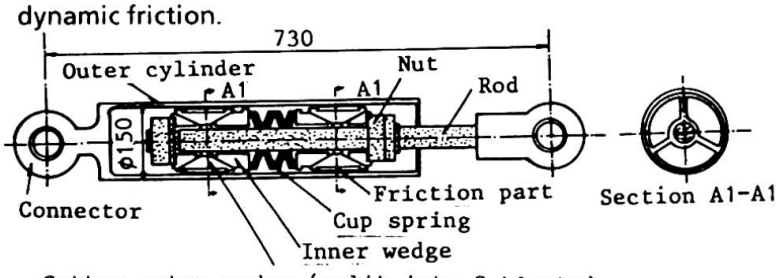

Fig. 1 Friction Damper's Mechanism

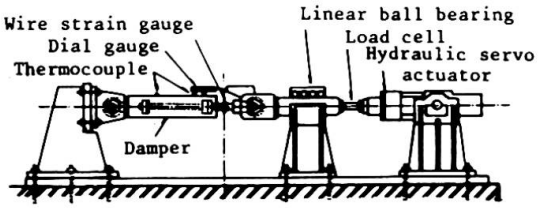

Fig. 2 Method of test

Amplitude δ: mm	Frequency f: Hz	Vibration speed*1 V: cm/sec.	N150*2 : cycle
1	1	0.63	15000
3	0.33	0.63	
5	5	15.71	250
10	0.33	2.09	
10	1	6.28	550
10	2	12.57	270
20	0.2	2.51	700
20	0.33	4.19	
20	0.5	6.28	500
20	2	25.13	
30	0.33	6.28	
38	0.33	8.38	350

*1 Speed at sliding displacement 0 position

*2 Repetition cycles at which outer cylinder temperature reaches T = 150°C

Table 1 Content of Vibration Test

Effects of vibration speed: Fig. 3 shows the effects of the vibration speed on restoring force characteristics. Fig. 5 shows the relationship between the vibration speed and the energy absorbed by the damper. It is evident that, as vibration speed v increases, the sliding load increases in the static friction range and drops a little in the dynamic friction range and that the damper's restoring force characteristics shift from a rectangular to concave shape. It is possible to consider, however, that such increase and decrease of the sliding load offset each other, so that the absorbed energy per cycle is nearly proportional to the sliding amount and is not affected by the vibration speed.

Effects of friction part temperature: Fig. 4 shows the effects of the friction part temperature on restoring force characteristics and Fig. 6 shows the relationship between the friction part temperature and the absorbed energy. It is evident that, as the friction part temperature rises, the sliding load increases a little in the static friction range and drops in the dynamic friction range. While the absorbed energy also drops as the temperature rises, the drop rate of the absorbed energy at friction part temperature T = 105°C is about 7% of that at T = 30°C.

Effects of vibration cycle: Test results showed the effects of the vibration cycle on restoring force characteristics. The friction part abrasion is a maximum of 0.1 mm in diameter after various vibration tests (total repetition is about 20,000 cycles). Considering that an abrasion of 0.1 mm represents a drop in frictional force of about 3% according to calculation, the friction damper can be judged as having sufficient durability under practical conditions.

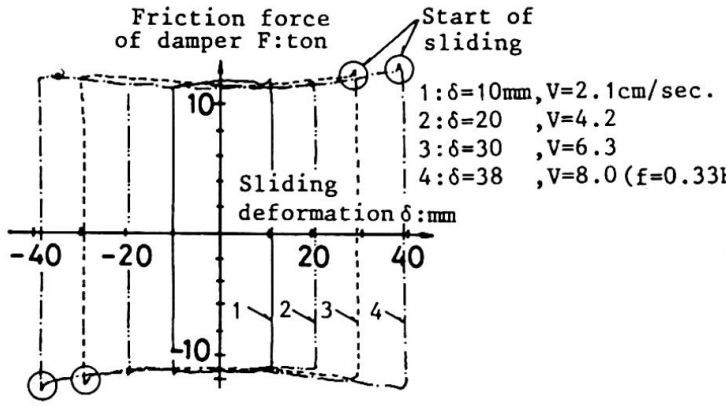

Fig. 3 Effects of Vibration Speed

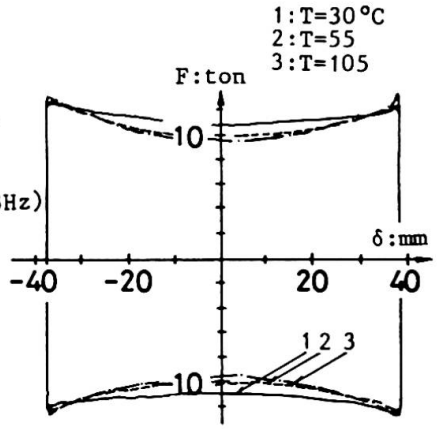

Fig. 4 Effects of Damper Temperature

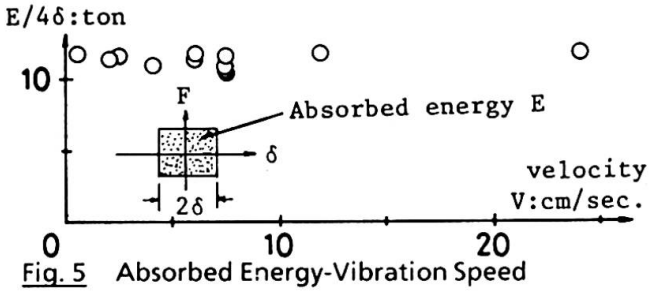

Fig. 5 Absorbed Energy-Vibration Speed

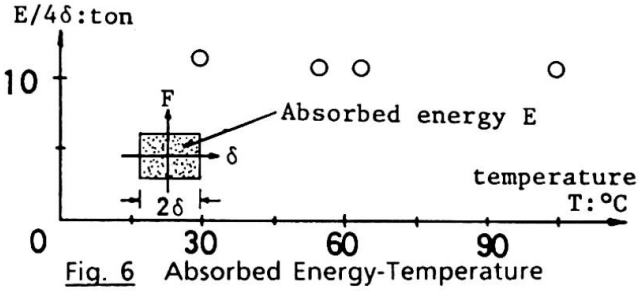

Fig. 6 Absorbed Energy-Temperature

3. EXPERIMENTS OF A FRAME WITH FRICTION DAMPER

After the tests of the friction damper itself, the static and dynamic loading tests for a steel frame with the friction damper were conducted. These tests were planned to ascertain the damper performance under practical conditions prior to putting it into use for a building.

3.1 Contents of Test

Fig. 7 shows the dimensions of the test frame. A damper of frictional force 10-ton and sliding length ± 60mm was installed between a upper steel beam and the top of a precast concrete wall. The precast concrete wall was fixed to the steel underbeam in 2 places at its bottom to create such a mechanism that a frictional force is generated in the damper via the precast concrete wall as the steel frame is subjected to story drift.

Loading Method: Fig. 7 shows the loading method. The steel frame was supported on the test bed, and static and dynamic horizontal forces were applied to it by means of an actuator.

Loading Procedure: Table 2 shows the loading procedure. For the dynamic loading test, the damper friction part's sliding amount and vibration period were taken as test parameters.

Measuring Procedure: The steel frame's story drift and the damper friction part's sliding displacement were measured with the dial gauge (D.G.) shown in Fig. 7 and the damper rod's strain (for detecting the damper's frictional force) was measured with the wire strain gauge (W.S.G.).

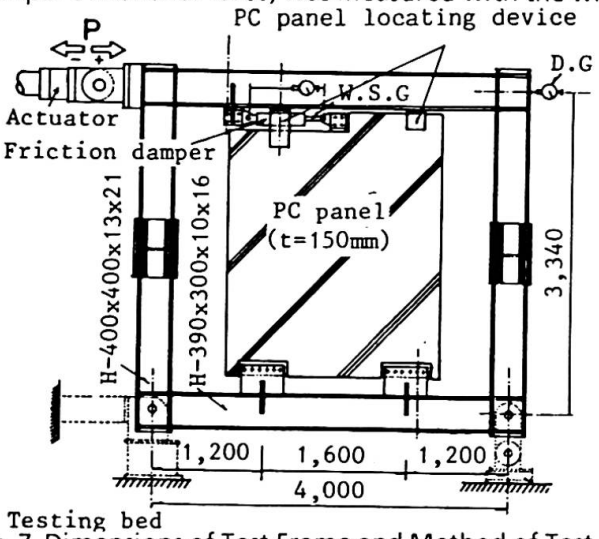

Fig. 7 Dimensions of Test Frame and Method of Test

Loading Step	Content of Loading
(1)	Static load: Gradually increased repetition of P = ±50 tonf
(2)	Dynamic load: Sine-wave vibration of T = 1, 2, 3, 4 sec., respectively, at δ = ±2, ±5, ±10, ±15 mm
(3)	Static load: Controlled from P = ±60 tonf to δ = 60 mm by the damper's sliding amount δ at △δ = 15 mm pitch
(4)	Dynamic load: Since-wave vibration of T = 3 sec. at δ = ±10, ±30 and T = 5 sec. at δ = ±50

Table 2 Loading Procedure

3.2 Test Results

Static Loading Test: Fig. 8 shows the test frame restoring force characteristics and Fig. 9 shows the damper frictional force-sliding displacement relationship. It is evident that the test frame restoring force characteristics are bi-linear as calculated even if the steel frame is in the elastic range. It can be seen that while the damper's frictional force is slightly more than 11 ton at the beginning of sliding (the ○ mark in the figure), it continues sliding at a stable frictional force of slightly more than 10 ton for the entire sliding length after starting to slide.

Dynamic Loading Test: Fig. 10 shows the test frame restoring force characteristics and Fig. 11 shows the damper frictional force-sliding displacement relationship as examples of their respective test results. Meanwhile, Fig. 12 shows the damper absorbed energy-vibration speed relationship.
It is evident that the test frame restoring force characteristics are bi-linear just as in the static loading test. There is no fluctuation in the frictional force of the damper at the beginning of sliding observed during the static loading test. The sliding load in the dynamic friction range drops in the vibration range of v = 6.2 cm/sec. or more. The damper restoring force characteristics shift from a rectangular to concave shape. The damper absorbed energy also tends to fall as vibration speed v rises. The drop rate of the absorbed energy at v = 8.7 cm/sec. was about 10% of that at v ≦ 3 cm/sec.

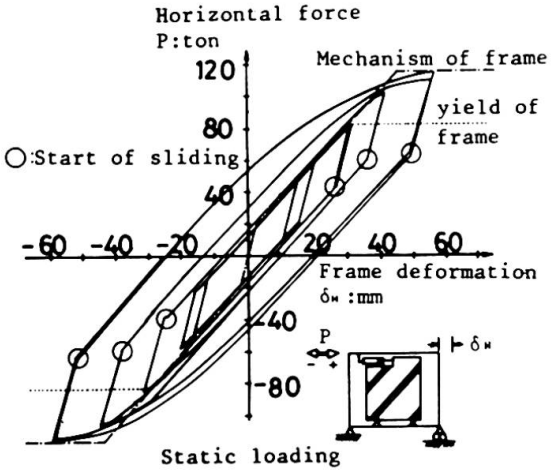

Fig. 8 Test Frame Restoring Force Characteristics

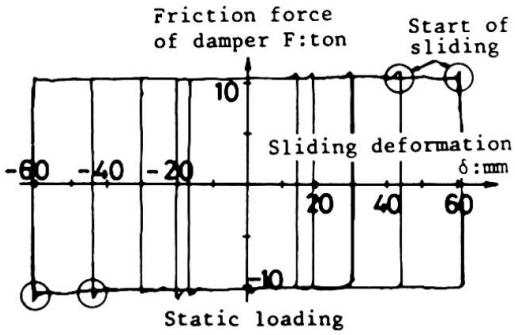

Fig. 9 Damper Characteristics

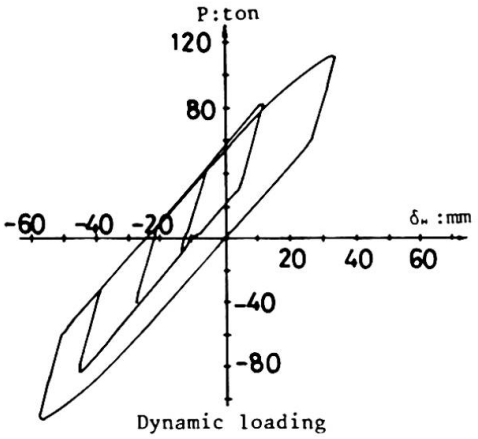

Fig. 10 Test Frame Restoring Force Characteristics

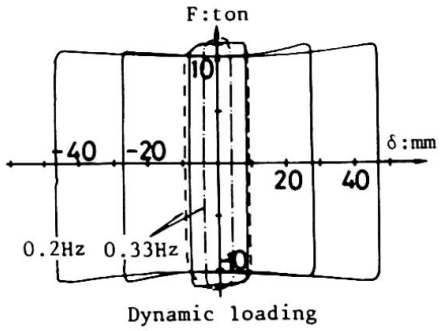

Fig. 11 Damper Characteristics

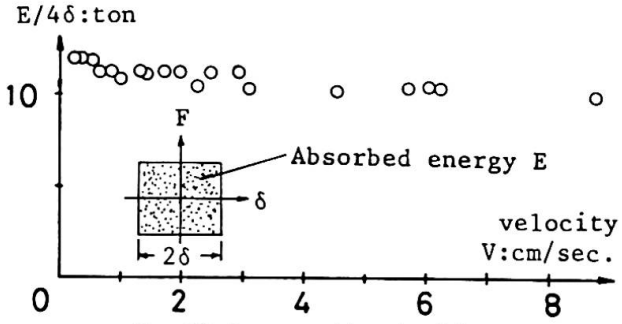

Fig. 12 Damper Absorbed Energy

4. APPLICATION OF FRICTION DAMPER TO HIGHRISE BUILDING

Friction dampers were installed in the Industrial Culture Center office building in Omiya, Japan, a 31-story steel-framed structure (Fig. 13).

The dampers were installed at the locations shown in Fig. 13. They were arranged almost symmetrically around the core wall. In the vertical direction, they were installed on all of the 1st ~ 31st floors. The number of pieces installed for each story was: X-direction, A1 x 4 pcs. and Y-direction, B2 x 2 pcs., for a total of 4 dampers each direction. Fig. 14 shows the details of the damper installation. Story drift is transmitted to the damper via the precast concrete wall, which generates a frictional force in the damper.

4.1 Dynamic Analysis

As the vibration model, a 32-mass shear model was used to represent the building. For the model, the design rigidity and restoring force of the frame was used. The damper restoring force characteristics were as described in Section 3.2. Table 3 shows the vibration model natural periods. While the initial rigidity increases due to the presence of the damper and the natural periods have become a little shorter, the difference is only about 10% in terms of the 1st period. As the input earthquake motion, El Centro 1940 NS was used. Table 4 shows the five types of intensity of input seismic motion adopted. In the case of small to medium earthquake motions, the building damping was estimated to be 1%, and in 25 & 50cm/sec. motions to be 2%.

Table 5 and Fig. 15 show the response results in the X-direction to seismic motions of 50~150 gal, while Table 5 and Fig. 16 show the results under ground motions of 25 & 50cm/sec. Therefore, the following conclusions are obtained.

(1) There is little difference in the response distribution between with or without dampers, so the response distributions look quite similar.

(2) Under small to medium earthquake motions, the overall response of the building is reduced about 20% by the effect of the dampers.

(3) The building overall response is reduced about 10% in the case of 25cm/sec. motions.

(4) In the case of 50 cm/sec. motions, the damper has little effect.

5. CONCLUSION

The above results show that a significant reduction in building sway was achieved, particularly in the case of small- to medium-scale earthquake motions. We have introduced above one example of a friction damper. Various mechanisms are conceivable for this type of energy absorption, and developments allowing this technique to be widely used can be expected in the future.

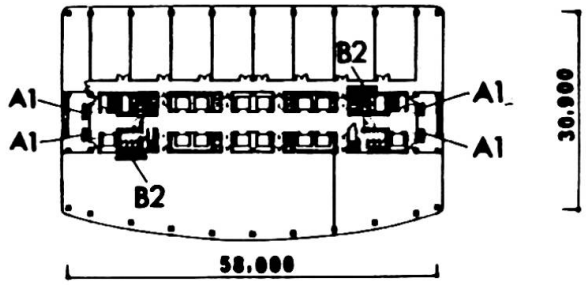

Fig. 13 Typical Floor Plan

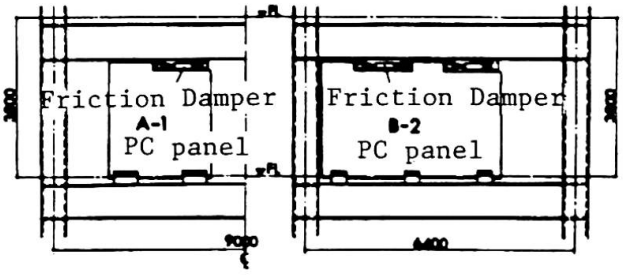

Fig. 14 Details of Damper Installation

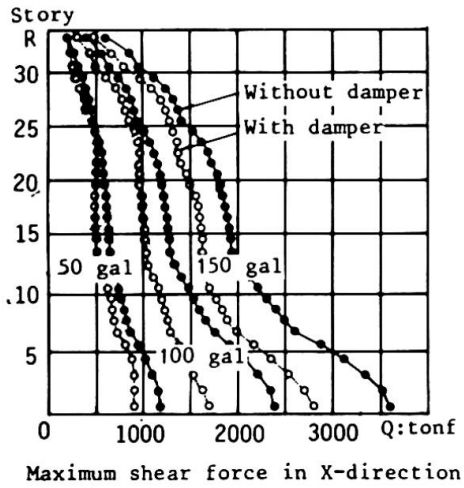

Fig. 15 Response Results at Ground Motion 50~150 gal

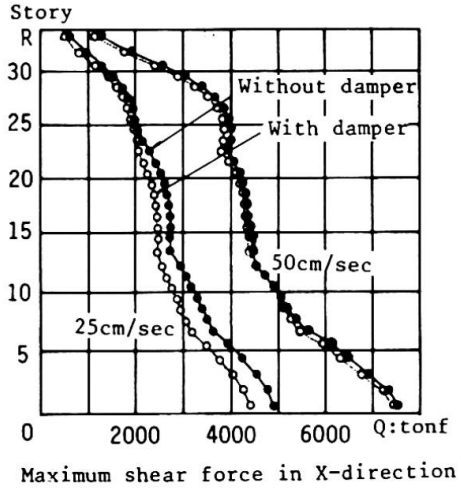

Fig. 16 Response Results at Ground Motion 25 & 50 cm/sec

		1st	2nd	3rd
X-direction	Without damper	3.12	1.17	0.77
	With damper	2.88	1.07	0.71
Y-direction	Without damper	3.06	1.12	0.73
	With damper	2.76	1.02	0.66

Table 3 Natural Periods (sec)

	Input Level	Acceleration (gal)	Building Damping (%)	Response Time (sec.)
1	Small to medium earthquake motions	50	1.0	20.0
2	Small to medium earthquake motions	100	1.0	20.0
3	Small to medium earthquake motions	150	1.0	20.0
4	25 cm/sec.	259	2.0	20.0
5	50 cm/sec.	518	2.0	20.0

Table 4 Input Seismic Motion

Input Level	50 gal			100 gal			150 gal			25 cm/sec.			50 cm/sec		
	Without	With	With/ Without	Without	With	With/ Without	Without	With	With/ Without	Without	With	With/ Without	Without	With	With/ Without
1st floor Q (t)	1206	925	0.77	2412	1730	0.72	3618	2830	0.78	4945	4470	0.90	7537	7450	0.99
10th floor Q (t)	746	638	0.86	1491	1180	0.79	2237	1730	0.77	3203	2800	0.87	4940	4920	1.00
1st floor δ (cm)	0.24	0.18	0.77	0.47	0.34	0.72	0.71	0.55	0.78	0.97	0.87	0.90	1.85	1.79	0.97
10st floor δ(cm)	0.36	0.30	0.86	0.71	0.56	0.79	1.07	0.82	0.77	1.53	1.33	0.87	2.73	2.71	0.99
Top displacement (cm)	8.07	6.40	0.79	16.1	12.8	0.79	24.2	19.9	0.82	35.8	32.8	0.92	66.7	66.0	0.99

Table 5 Response Results (X-Direction)